Mesoporous Alumina and Aluminosilica with Pd and Pt Nanoparticles: Structure and Catalytic Properties

Lyudmila M. Bronstein,*[,†,‡] Dmitri M. Chernyshov,[‡] Robert Karlinsey,[†] Josef W. Zwanziger,[†] Valentina G. Matveeva,[§] Esther M. Sulman,[§] Galina N. Demidenko,[§] Hans-Peter Hentze,[||] and Markus Antonietti[||]

Chemistry Department, Indiana University, Bloomington, Indiana 47405, A.N. Nesmeyanov Institute of Organoelement Compounds, Moscow 117813, Russia, Tver Technical University, Tver 170000, Russia, and Max Planck Institute of Colloids and Interfaces, D-14424 Potsdam, Germany

Received December 4, 2002. Revised Manuscript Received April 25, 2003

Cationic and anionic microgels based on sulfonated polystyrene and poly(ethylmethacryltetramethylammonium chloride) and containing Pd and Pt nanoparticles were used as templates along with polystyrene-*block*-poly(ethylene oxide) block copolymers for casting nanoporous alumina and aluminosilica with nanoparticles. The Pt-nanoparticle-containing aluminosilica consists of interpenetrating pores and Pt particles of 7 nm in diameter (by X-ray diffraction) located in the interpore channels. Pd nanoparticles are smaller and partially block the pore entrances of Pd-nanoparticle-containing aluminosilica, decreasing the porosity. Metal-particle-containing aluminas templated both over cationic and anionic microgels consist of an interpenetrating pore system and alumina nanowires (2−3 nm in diameter and about 40 nm in length) along with Pd or Pt nanoparticles. This combination creates higher mesoporosity than for aluminosilicas. The ^{27}Al MAS NMR spectra of metal-nanoparticle-containing alumina show two distinct sites at 0 and 65 ppm independently of metal or microgel types, indicating octahedral and tetrahedral coordination, respectively; the octahedral species strongly prevail. The aluminum spectra of all aluminosilica samples show a more complicated picture, with octahedral and tetrahedral aluminum along with probable pentacoordinated species. The catalytic properties of Pd(Pt)-nanoparticle-containing aluminas and aluminosilicas were studied in partial hydrogenation of three amphiphilic acetylene alcohols having a different length of the hydrophobic tail. The aluminosilicas showed low activity and selectivity for all substrates, while Pd-particle-containing aluminas displayed high activity and selectivity, especially for acetylene alcohol with the longest aliphatic tail (dehydroisophytol, acetylene alcohol C_{20}).

Introduction

Synthesis and study of mesoporous materials containing nanoparticles represent a fast developing area of nanoscience and nanotechnology. This interest is stimulated by several possible application areas: catalytic,[1−3] magnetic,[4,5] and optical materials.[6−8] Nanoparticles offer a huge specific surface area and superior catalytic properties in a variety of chemical reactions. Their location in the pores of porous materials results in their stabilization and modification of their properties (surface modification). At least six general approaches for synthesis of mesoporous materials with nanoparticles located in pores have been identified, including impregnation,[9] interaction with functional groups of mesoporous solids (for example, silanol groups),[10−12] chemical vapor deposition inside the pores,[13] template ion exchange with transition metal cations,[14] use of prefabricated nanoparticles,[15] and templating over metal-containing templates. The latter avenue allows controlling both particle size and pore size via the structure of the same template. This approach was first reported in

* To whom correspondence should be addressed. E-mail: lybronst@indiana.edu.
† Indiana University.
‡ A.N. Nesmeyanov Institute of Organoelement Compounds.
§ Tver Technical University.
|| Max Planck Institute of Colloids and Interfaces.

(1) Ying, J. Y.; Mehert, C. P.; Wong, M. S. *Angew. Chem., Int. Ed.* **1999**, *38*, 56.
(2) Morey, M. S.; Bryan, J. D.; Schartz, S.; Stucky, G. D. *Chem. Mater.* **2000**, *12*, 3435.
(3) Liu, J.; Feng, X.; Fryxel, G. E.; Wang, L.-Q.; Kim, A. Y.; Gong, M. *Adv. Mater.* **1998**, *10*, 161.
(4) Schnider, J. J.; Czap, N.; Hagen, J.; Engstler, J.; Ensling, J.; Gütlich, P.; Reinoehl, U.; Bertagnolli, H.; Luis, F.; de Jongh, L. J.; Wark, M.; Grubert, G.; Hornyak, G. L.; Zanoni, R. *Chem. Eur. J.* **2000**, *6*, 4305.
(5) Jung, J.-S.; Chae, W.-S.; McIntyre, R. A.; Seip, C. T.; Wiley, J. B.; O'Connor, C. J. *Mater. Res. Bull.* **1999**, *34*, 1353.
(6) Moller, K.; Bein, T. *Chem. Mater.* **1998**, *10*, 2950.
(7) Shi, H.; Zhang, L.; Cai, W. *J. Appl. Phys.* **2000**, *87*, 1572.
(8) Powers, K. W.; Hench, L. L. *Ceram. Trans.* **2000**, *101*, 253.
(9) Plyuto, Y.; Berquer, J.-M.; Jacquiod, C.; Ricolleau, C. *Chem. Commun.* **1999**, 1653.
(10) Zhang, W.-H.; Shi, J.-L.; Wang, L.-Z.; Yan, D.-S. *Chem. Mater.* **2000**, *12*, 1408.
(11) Lebeau, B.; Fowler, C. E.; Mann, S.; Farcet, C.; Charleux, B.; Sanchez, C. *J. Mater. Chem.* **2000**, *10*, 2105.
(12) Zhang, L.; Sun, T.; Ying, J. Y. *Chem. Commun.* **1999**, 1103.
(13) Mehnert, C. P.; Weaver, D. W.; Ying, J. Y. *J. Am. Chem. Soc.* **1998**, *120*, 12289.
(14) Iwamoto, M.; Tanaka, Y. *Catal. Surv. Jpn.* **2001**, *5*, 25.
(15) Mukherjee, P.; Sustry, M.; Kumar, R. *PhysChemComm* **2000**, *3*.

10.1021/cm021776x CCC: $25.00
Published on Web 05/22/2003

refs 16 and 17. When metal nanoparticles are located in the block copolymer micelle cores[16] or in microgels[17] and these polymeric systems are used as templates for silica casting, particles are exactly placed in the pores of mesoporous solids after template removal. Reference 17 describes the use of spherical microgels as nanosized exotemplates for synthesis of metal colloids[18] and as endotemplates [along with the block copolymer (polystyrene-*block*-poly(ethylene oxide), PS-*b*-PEO template] during casting of the mesoporous sol−gel silicas. After calcination the block copolymer template provides the interpenetrating mesopore structure and good access to pores formed due to microgels. As shown in ref 17, metal particles remain discrete after calcination and access to the nanoparticle surfaces is ensured by the mesopore system. Use of metal-particle-containing templates seems to be promising for robust control over nanoparticle growth in mesoporous solids. Another example of this kind of template is dendrimers loaded with Cu^{2+} ions.[19] As is well-known, poly(propylene)imine dendrimer (DAB-Am-64) serves as a nanoreactor for well-controlled nanoparticle formation.[20] However, when such dendrimers alone (without any co-template) are used as silica templates,[19] well-developed interpenetrating pore structure, which is required for catalytic application, is not formed. The above-mentioned disadvantages seem to be overcome in cyclodextrin-based porous silica.[21] When cyclodextrins are used as templates for silica casting,[22] they form interpenetrating "worm-type" pore structures (due to self-assembly in concentrated solutions) resembling those obtained after block copolymer templating. If hydrophobic metal-containing inclusion compounds are used along with cyclodextrins as templates, metal is incorporated first within cyclodextrins and then within the pores of mesoporous material after templating. However, as particles are formed during calcination, their irregular growth and penetration in interpore channels cannot be avoided. In our opinion, polymer templates with preformed nanoparticles are superior from the viewpoint of control over particle size and overall properties of the materials, especially catalytic ones. The catalytic properties of mesoporous materials with embedded nanoparticles are mainly governed by the type of the inclusion (nanoparticle). All catalytic reactions, which are normally carried out for the particular metals or alloys, can be performed with mesoporous solids containing nanoparticles. The important advantage of mesoporous oxides is their stability at high temperatures. Due to this feature, mesoporous oxides with nanoparticles can be successfully used as catalysts in reactions where nanoparticles embedded in polymeric systems cannot be employed. Another plausible advantage of the mesoporous catalysts is an appropriate use of pores as nanoreactors of a certain size. This can be applicable to a catalytic reaction with large molecules or to a cyclization reaction where pore size and shape will influence the reaction path.[23] In this paper we continue the avenue suggested by us in ref 17 using cationic and anionic microgels with metal nanoparticles as templates. Here, we report synthesis and structure of mesoporous alumina and nanoporous aluminosilica with Pd and Pt nanoparticles and their catalytic properties in selective hydrogenation of long-chain alcohols. To study the influence of substrate size on catalytic properties, we chose three amphiphilic substrates having a different length of the hydrophobic tail, acetylene alcohols C_5 (2-methyl-3-butyn-2-ol, dimethylethynylcarbinol, DMEC), C_{10} (3,7-dimethyl-6-octen-1-yn-3-ol, dehydrolinalool, DHL), and C_{20} (3,7,11,15-tetramethyl-1-hexadecyn-3-ol, dehydroisophytol, DHIP), and studied their hydrogenation to corresponding olefin alcohols, 2-methyl-3-buten-2-ol (dimethylvinylcarbinol, DMVC), 3,7-dimethyl-1,6-octadien-3-ol (linalool, LN), and 3,7,11,15-tetramethyl-1-hexadecen-3-ol (isophytol, IP) (Scheme 1). DMVC, LN, and IP are intermediate products in vitamins A, E, and K synthesis.[24−26] LN is a fragrance used in perfumes and cosmetic preparations.[27−29]

Experimental Procedures

Materials. $PdCl_2$, $Pt(NH_3)_4(NO_3)_2$, K_2PtCl_4, and Na_2PdCl_4 were obtained from Aldrich and used as received. Aluminum tri-*sec*-butoxide and $AlSi(OR)_x$ (Aldrich) were used without further purification. Polystyrene-*block*-poly(ethylene oxide), PS-*b*-PEO, block copolymer (SE 1010) was obtained from Goldshmidt AG and used as received. 2-Propanol (Aldrich) was distilled. DMEC, DHL, and DHIP (OAO Belgorodvotaminy, Belgorod, Russia) were distilled under vacuum before use. Pyridine of spectrophotometric grade was purchased from ACROS and used as received. Water was deionized in a Milli-Q purification system.

Synthesis. *Synthesis of Polystyrene-Sulfate Anionic Microgels.* Synthesis of polystyrene-sulfate anionic microgels (cross-linking density 1/40, degree of sulfonation 90−95%, particle diameter 90 nm) containing ionogenic $-SO_3^-$ groups and ethylmethacryltetramethylammonium chloride cationic microgels (cross-linking degree 1/72, particle size 91 nm) is described elsewhere.[17,30]

Incorporation of Metal Ions. Incorporation of metal ions inside the microgels was performed by mixing of microgel solution (1.0 g/L in water) with a corresponding metal salt with a molar ratio [microgel charged group]:M = 3:1 and stirring overnight. Anionic gels were reacted with metal salts, $PdCl_2$ and $Pt(NH_3)_4(NO_3)_2$, giving desired metal cations, while cationic gels were allowed to ion exchange with Pd and Pt anions (K_2PtCl_4 and Na_2PdCl_4). Replacement of H^+ or Cl^- ions with metal ions, driven by entropy (as the metal ions are bivalent), results in metalation of microgels. The metalated microgels were then reduced by using $NaBH_4$ (3-fold excess toward metal

(16) Bronstein, L.; Krämer, E.; Berton, B.; Burger, C.; Förster, S.; Antonietti, M. *Chem. Mater.* **1999**, *11*, 1402.
(17) Whilton, N. T.; Berton, B.; Bronstein, L.; Hentze, H.-P.; Antonietti, M. *Adv. Mater.* **1999**, *11*, 1014.
(18) Antonietti, M.; Groehn, F.; Hartmann, J.; Bronstein, L. *Angew. Chem., Int. Ed. Engl.* **1997**, *36*, 2080.
(19) Velarde-Ortiz, R.; Larsen, G. *Chem. Mater.* **2002**, *14*, 858.
(20) Zhao, M.; Sun, L.; Crooks, R. M. *J. Am. Chem. Soc.* **1998**, *120*, 7355.
(21) Han, B.-H.; Polarz, S.; Antonietti, M. *Chem. Mater.* **2001**, *13*, 3915.
(22) Polarz, S.; Smarsly, B.; Bronstein, L.; Antonietti, M. *Angew. Chem., Int. Ed.* **2001**, *40*, 4417.
(23) Vartuli, J. C.; Shih, S. S.; Kresge, C. T.; Beck, J. S. *Stud. Surf. Sci. Catal.* **1998**, *117*, 13.
(24) Duca, D.; Frusteri, F.; Parmaliana, A.; Deganello, G. *Appl. Catal. A* **1996**, *146*, 269.
(25) Schbib, N. S.; Garcia, M. A.; Gigola, C. E.; Errazu, A. F. *Ind. Eng. Chem. Res.* **1996**, *35*, 1496.
(26) Pena, J. A.; Herguido, J.; Guimon, C.; Monzon, A.; Santamaria, J. *J. Catal.* **1996**, *159*, 313.
(27) Perucci, S.; Cioni, P. L.; Cacella, A.; Macchioni, F. *Med. Vet. Entomol.* **1997**, *11*, 300.
(28) Pattnaik, S.; Subramanyam, V. R.; Bapaji, M.; Kole, C. R. *Microbios* **1997**, *89*, 39.
(29) Nakatsu, T.; Van Loveren, A. G.; Kang, R. K. L.; Cilia, A. T. U.S. Patent 5965518, 1999; *Chem. Abstr.* 131:276814 AN 1999:655936.
(30) Antonietti, M.; Briel, A.; Foerster, S. *J. Chem. Phys.* **1996**, *105*, 7795.

Scheme 1. Hydrogenation Paths of DMEC, DHL, and DHIP

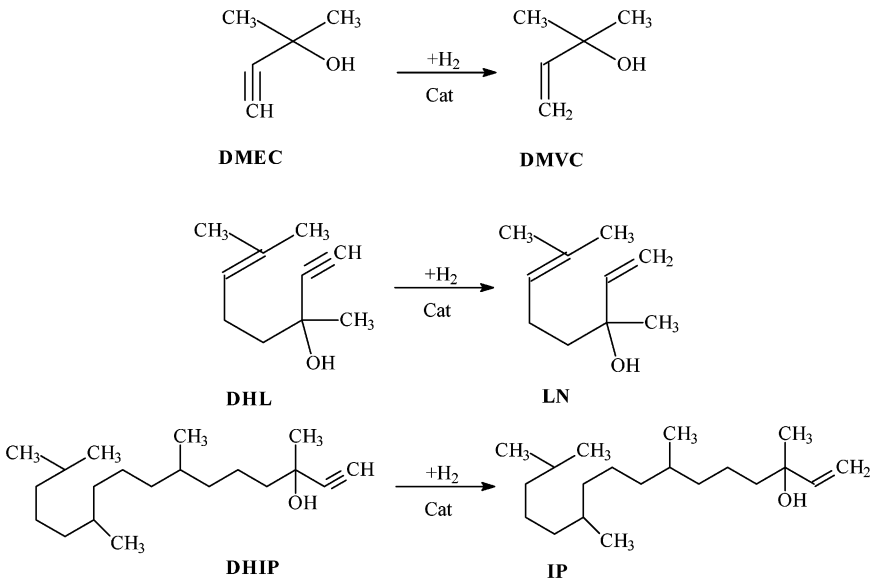

ions) and concentrated using an Amicon ultrafiltration device to 20 wt % solid content. The latter procedure was accompanied by purification of metal-particle-microgel solution from any metal particles located outside the microgel particles (the size of the latter is smaller than filter pore size). Typically, to prepare ≈3 mL of the concentrated solution, initially 100 mL of microgel solution was used. Finally, a pH of the concentrated microgel solution was adjusted between 2 and 7.

Synthesis of Nanoporous Solids. Synthesis of nanoporous solids was performed by a modification of a method described in ref 17. Typically, 2 g of metal-containing microgel dispersion was mixed upon cooling (5 °C) with solution containing 2 g of SE 1010 and 4 g of the corresponding metal alkoxide dissolved in 5 mL of tetrahydrofuran. Vigorous stirring of reaction media and consequent evaporation of alcohols (hydrolysis and condensation products) at full vacuum result in the formation of dark-gray powders. Removal of organic template was performed by calcination at 500 °C in Ar for 6 h and then in O_2 for 12 h.

In this paper the following notations are used: A-Pd-NCM-[Al] stands for anionic (A) microgel with Pd (Pd) nanoparticles used for templating of alumina ([Al]). C-Pd-NCM-[Al] stands for cationic (C) microgel with Pd (Pd) nanoparticles used for templating of alumina ([Al]). [AlSi] stands for aluminosilica.

Characterization. X-ray diffraction (XRD) patterns were collected on an Enraf-Nonius PDS120 powder diffractometer. A FR590 generator was used as a source for Cu Kα radiation (with a Ni filter). Transmission electron microscopy (TEM) images were acquired on a Zeiss EM 912Ω at an acceleration voltage of 120 kV. Samples were ground in a ball mill and suspended in acetone. One droplet of the suspension was applied to a 400-mesh carbon-coated copper grid and left to dry in air.

Nitrogen sorption experiments were carried out at liquid nitrogen temperature using a Micromeritics Gemini instrument. Samples were degassed at 100 °C in vacuo for 12 h prior to investigation.

Solid-state NMR measurements were performed on a Bruker DSX 400-MHz NMR spectrometer, using a 4-mm magic angle sample spinning (MAS) probe. Rotation frequencies are indicated on the spectra shown below and were stabilized with an active feedback spin-rate controller.

FT-IR spectra were recorded with a Nicolet 510P spectrometer in the range 4000−400 cm^{-1}. Pyridine was added to MCPM-templated samples after their prior treatment at 150 °C for 1 h in a vacuum in a Schlenck tube. After 1-h pyridine adsorption at 150 °C, the sample was evacuated at 200 °C to ensure removal of the hydrogen-bound pyridine and then filled with argon.[31] The spectra were collected at room temperature in nitrogen.

Table 1. Dependence of Reaction Rate on a Stirring Rate in Hydrogenation of DHL to LN with MNCM-Templated Nanoporous Alumina and Aluminosilica[a]

	specific rate (mol mg of Pd^{-1} min^{-1}) with stirring rate, shakes per minute				
	480	760	920	960	1040
A-Pd-NCM-[AlSi]	2.1	3.0	3.8	3.8	3.8
A-Pd-NCM-[Al]	7.6	11.8	16.3	16.3	16.3

[a] Reaction conditions: 0.013 mol of DHL and 0.1 g of catalyst in 30 mL of 2-propanol at 70 °C.

Hydrogenation. The catalytic reactions have been carried out in a glass batch isothermal reactor installed in a shaker (maximum 1040 shakes per minute) and connected to a gasometric buret. The reactor was equipped with two inlets: for catalyst, solvent, and substrate loading and for hydrogen feeding. Before the substrate was charged into the reactor, the catalyst was pretreated with H_2 for 60 min at 70 °C. The catalyst amount (C_c) was varied. The experiments were carried out at atmospheric pressure. Variation of shaking intensity (stirring rate) for two representative catalysts (Table 1) showed that, in the range 920−1040 shakes per minute, the reaction rate is independent of the stirring rate, so the catalytic systems are free from external diffusion limitations. All experiments were carried at 960 shakes per minute.

Analysis of the reaction mixture was carried out by gas chromatography (GC) using chromatograph "CHROM - 5" with FID and glass column 3 m/3 mm. The column was filled with solid phase "Chromaton N" (0.16−0.20 mm) saturated with carbowax, 20 M (10% of liquid phase to support weight).

Results and Discussion

Structure of Pd- and Pt-Nanoparticle-Containing Nanoporous Solids. TEM images of nanoporous alumina and aluminosilica templated over metal-nanoparticle-containing (cationic and anionic) microgels (MNCM) are presented in Figures 1 and 2.

For aluminosilica, TEM (Figure 1) reveals a continuous nanoporous network containing metal nanoparticles (shown by arrows) or particle ensembles (circled) sta-

(31) Blumenfeld, A. L.; Fripiat, J. J. *Top. Catal.* **1997**, *4*, 119.

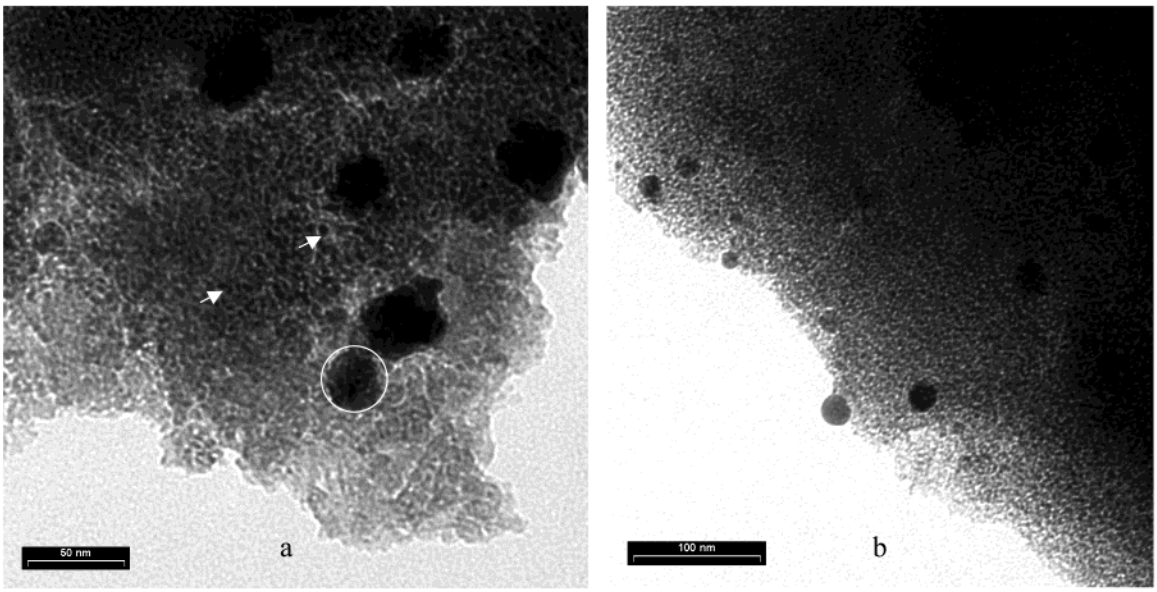

Figure 1. TEM images of MNCM-templated aluminosilica samples: C-Pt-NCM-[AlSi] (a) and A-Pd-NCM-[AlSi] (b). Arrows show discrete particles, while circles show particle aggregates.

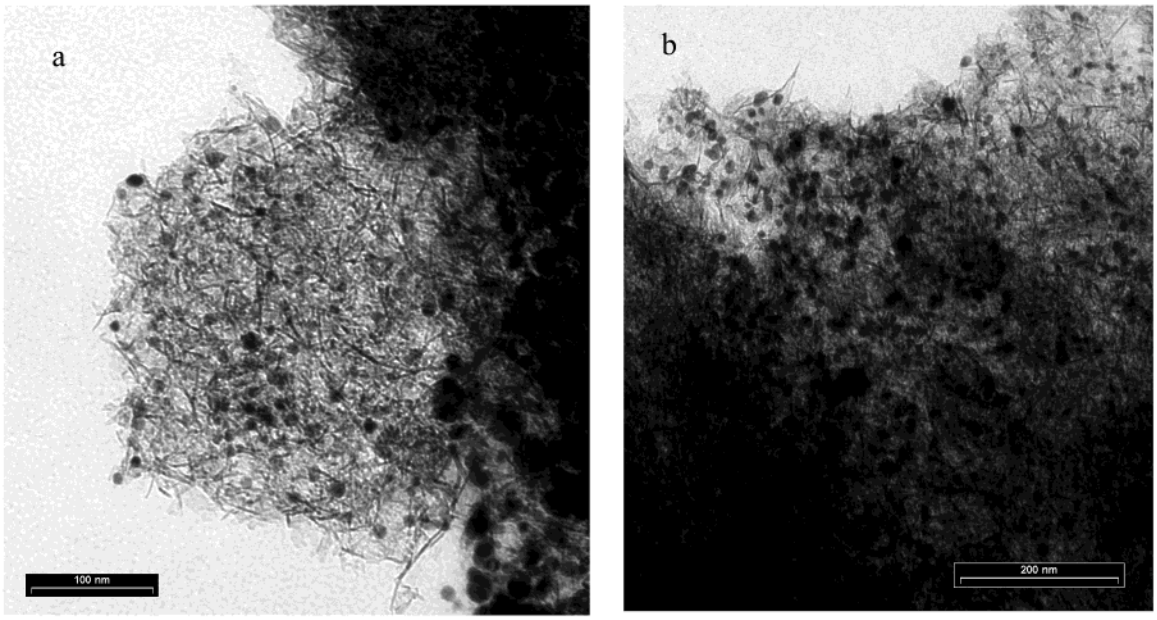

Figure 2. TEM images of MNCM-templated alumina samples: C-Pd-NCM-[Al] (a) and C-Pd-NCM-[Al] (b).

tistically embedded in the porous solid. This structure closely resembles the one of the MNCM-templated silica described by us earlier[17] and generally does not depend on the microgel type (cationic or anionic). As discussed in ref 17, nanoparticles formed in microgels do not aggregate during the sol−gel process followed by calcination due to reliable stabilization by a microgel network and penetration of forming silica network within microgels. This results in the material where most of the nanoparticles stay intact and the average particle size does not change after calcination.[17] A similar situation is observed for aluminosilica. By XRD data presented in Figure 3a, the average Pt crystallite size (calculated for $2\theta = 39.8°$ (111) using the Scherrer equation) in C-Pt-NCM-[AlSi] is 7 nm. A strong broad peak centered at $2\theta = 21°$ is assigned to amorphous aluminosilica. Inspection of the TEM micrograph of this sample (Figure 1a) allows one to distinguish a high population of particles with diameters of 4−6 nm along with larger particle ensembles reaching 40 nm. The latter, in turn, consists of smaller discrete particles. In the case of C-Pd-NCM-[AlSi] (Figure 1b), the nanoporous material structure is analogous, but the greater part of the particles are 3−5 nm in size. The XRD pattern (Figure 3b) shows very weak reflections that can be assigned to PdO crystallites 10−12 nm in size [calculated for $2\theta = 41.9°$ (110)]. This allows us to assume that smaller particles are rather amorphous, while large-particle ensembles consist of crystalline particles. The shape of the nitrogen adsorption−desorption isotherms for aluminosilica samples (Figure 4a,b) showing large adsorption at low relative pressures and small hysteresis loops are evidence of high microporosity and low mesoporosity of these samples. The BJH (Barrett, Joyner, and Halenda) pore distribution confirms the lack of pores larger than 4 nm. The BJH

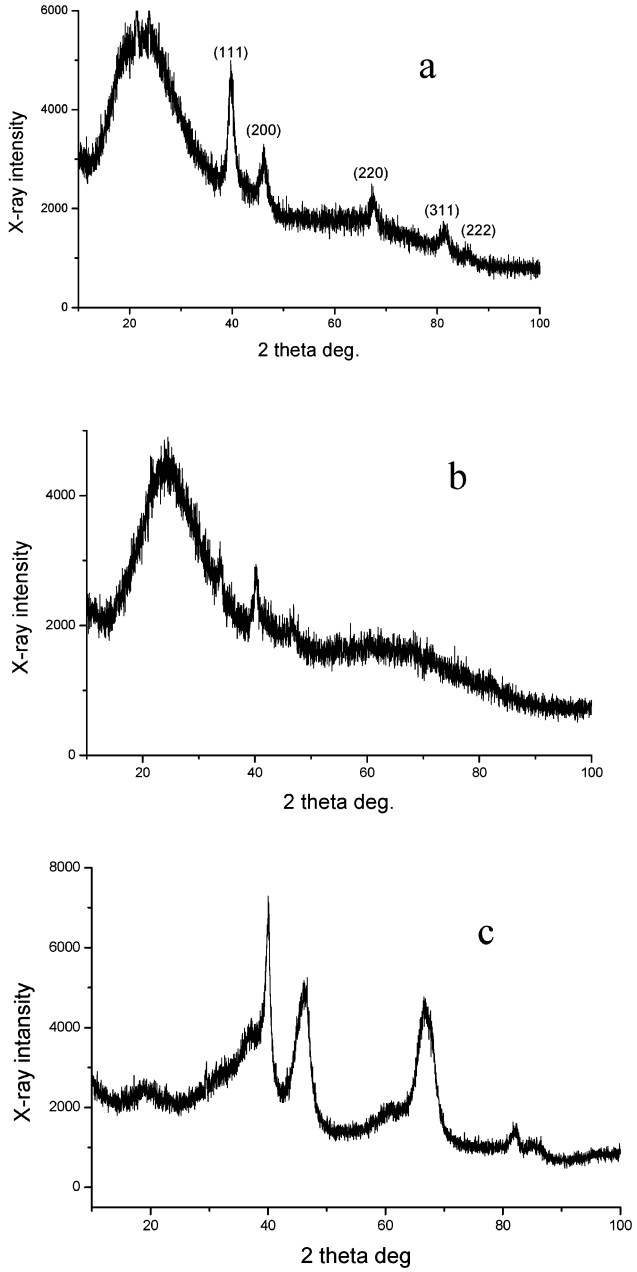

Figure 3. XRD profiles of C-Pt-NCM-[AlSi] (a), C-Pd-NCM-[AlSi] (b), and A-Pd-NCM-[Al] (c) samples.

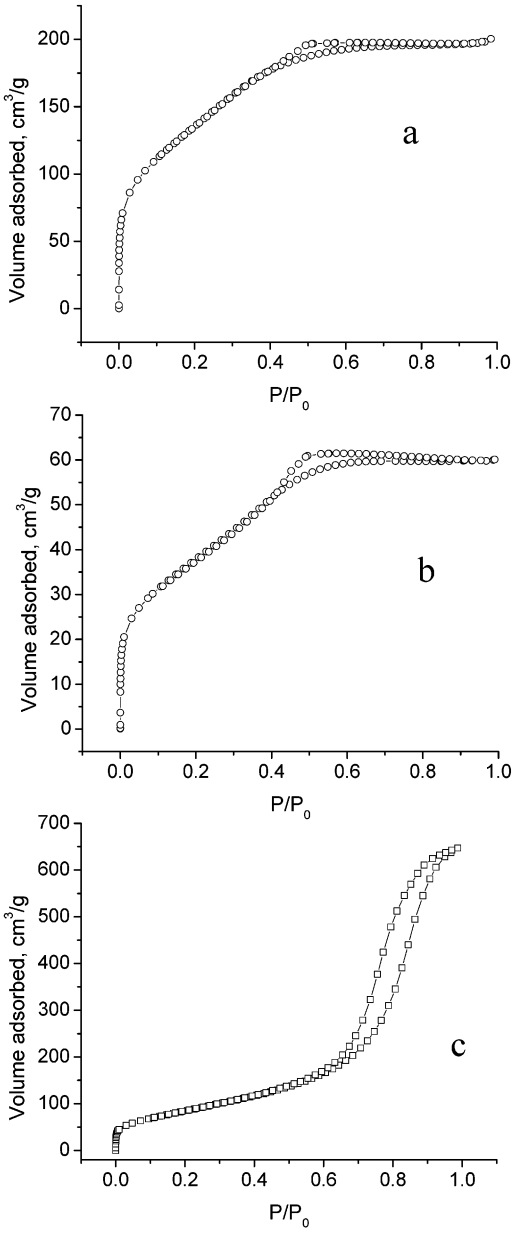

Figure 4. BET nitrogen isotherms of C-Pt-NCM-[AlSi] (a), C-Pd-NCM-[AlSi] (b), and C-Pd-NCM-[Al] (c) samples.

desorption average pore diameter shows almost no dependence on metal (Pd, Pt) or microgel types and varies in the range of 2.6−2.9 nm. Taking into consideration that the average pore diameter of mesoporous silica templated over the same block copolymer (SE 1010) in the absence of microgels measures about 3 nm,[32] one can conclude that PdO or Pt nanoparticles do not influence the aluminosilica pore structure. On the other hand, for C-Pt-NCM-[AlSi], the BET (Brunauer−Emmet−Teller) surface area is 495 m^2/g, while for C-Pd-NCM-[AlSi], the BET surface is only 138 m^2/g. One might presume that, in C-Pt-NCM-[AlSi], larger particles are located in the interpore defects and do not block meso- or micropores, while in C-Pd-NCM-[AlSi], metal particles are smaller than some pores and are able to block smaller pore entrances, decreasing the porosity.

Unlike aluminosilica, MNCM-templated alumina shows little similarity to MNCM-templated silica. The mesoporous alumina consists of two components: a porous network and alumina nanofibers (2−3 nm in diameter and about 40 nm in length); the latter are intimately embedded in the porous network (Figure 2). This combination creates larger mesoporosity and diminishes microporosity as demonstrated by the nitrogen adsorption−desorption isotherms (Figure 4c). The C-Pd-NCM-[Al] sample has a mean pore diameter of 8.0 nm (from BJH) and total BET surface area of 311 m^2/g, while for the A-Pd-NCM-[Al] sample, the BET surface area is 227 m^2/g and the mean pore diameter is 3.8 nm. Presumably, cationic microgels associate with the growing anionic alumina species, causing formation of larger pores than in the anionic microgels. The lack of this trend for aluminosilica confirms our hypothesis that

(32) Goltner, C. G.; Henke, S.; Weissenberger, M. C.; Antonietti, M. *Angew. Chem., Int. Ed.* **1998**, *37*, 613.

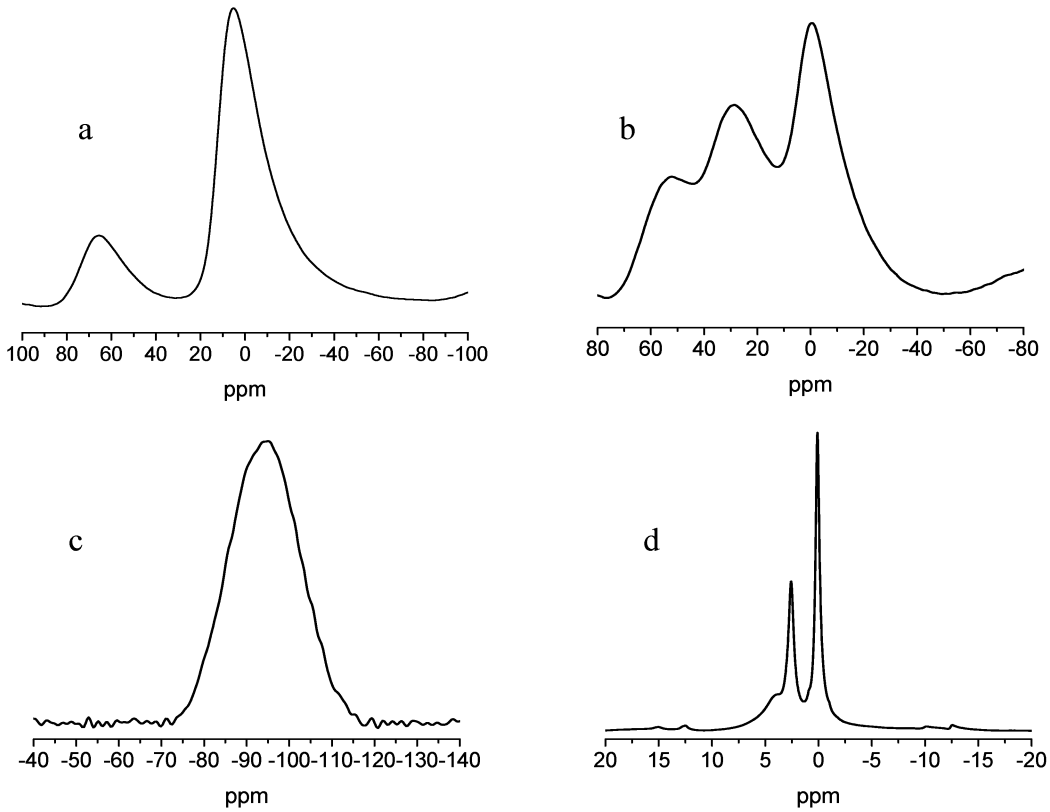

Figure 5. ^{27}Al MAS NMR spectra of A-Pd-NCM-[Al] (a) and A-Pd-NCM-[AlSi] (b); ^{29}Si CP-MAS NMR (c) and ^{1}H MAS NMR (d) spectra of A-Pd- NCM-[AlSi].

alumina species are involved in the interaction. Metal nanoparticles, varying slightly in size depending on the metal and microgel types, are incorporated in the mesoporous alumina. From TEM data, in A-Pd-NCM-[Al] the Pd nanoparticles are in the range 6−19 nm (Figure 2a), while for C-Pd-NCM-[Al], the particle diameter varies from 6 to 27 nm (Figure 2b). At the same time, the micrographs show smaller nanoparticles (of about 2 nm in diameter) included in the alumina nanofibers. XRD profiles of these samples are similar and show a complicated pattern that can result from superposition of reflections characteristic of crystalline alumina and Pd (or PdO) nanoparticles. Formation of alumina nanofibers using hydrolysis of $NaAlO_2$ in the presence of nonionic PEO surfactants (Tergitol 15S-*n*) followed by calcination at 500 °C was reported recently in ref 33. The resulting material, γ-Al_2O_3, shows an XRD pattern that strongly resembles the one shown in Figure 3c except that reflection intensities differ. The latter can be caused by superposition from Pd or PdO crystallites. This complicated pattern does not allow us to extract Pd (or PdO) particle sizes from XRD data. Similarities in sizes and shapes of alumina nanofibers reported in ref 33 and described in this paper allow us to conclude that nanofiber formation is not catalyzed by Pd or Pt nanoparticles as might be expected because the majority of alumina nanofibers in our samples include metal or metal oxide nanoparticles. Apparently, SE 1010 block copolymer behaves similarly to nonionic PEO surfactant[33] in inducing nanofibers formation. Moreover, the larger molecular weight of both PS and PEO blocks in SE 1010 compared to Tegritols described in ref 33 clearly makes no impact on the nanofiber formation. We believe that the explanation offered in ref 33 is viable in our case as well: one can assume that PEO units of block copolymer surfactant interact with a surface of growing boehmite (AlOOH) crystallites via hydrogen bonding, affording growth along one direction.

The local structure of the nanoporous aluminosilica and alumina was studied with solid-state NMR. The silicon and aluminum spectra are shown in Figure 5. The ^{27}Al MAS NMR spectra of MNCM-templated alumina (independently of metal or microgel types) show two distinct sites at 0 and 65 ppm, indicating octahedral and tetrahedral coordination, respectively; the octahedral species strongly prevail (Figure 5a). The aluminum spectra of all aluminosilica samples show more complicated patterns (Figure 5b). Again, the most pronounced peak at 0 ppm belongs to octahedral (six-coordinated) aluminum. The weakest peak at 53 ppm should be assigned to tetrahedral Al in aluminosilica.[34] The intermediate signal with a maximum centered at 28 ppm can be assigned to either a nonframework tetrahedral Al species in a highly distorted environment or pentacoordinate species as reported in ref 35. The ^{29}Si cross-polarization (CP)-MAS NMR spectra of aluminosilica samples (a representative spectrum is given in Figure 5c) shows a single, broad resonance with a peak maximum at 95 ppm, which can be assigned to Q^4 Si species (no OH groups connected to Si) where Si atoms are surrounded by 2 Si and 2 Al atoms (connected

(33) Zhu, H. Y.; Riches, J. D.; Barry, J. C. *Chem. Mater.* **2002**, *14*, 2086.

(34) Chaudhari, K.; Das, T. K.; Chandwadkar, A. J.; Sivasanker, S. *J. Catal.* **1999**, *186*, 81.

(35) Ray, G. J.; Meyers, B. L.; Marshall, C. L. *Zeolites* **1987**, *7*, 307.

Table 2. Catalytic Activity and Selectivity of MNCM-Templated Nanoporous Alumina and Aluminosilica in Hydrogenation of DHL to LN[a]

catalyst notation	catalyst amount, g	elemental analysis data on metal, %	specific rate, mol mg of Pd^{-1} min^{-1}	product ratio, wt. % DHL/LN/DiHL[b]	selectivity, %
A-Pd-NCM-[Al]	0.10	1.40	16.3	1.0/89.1/9.9	90
A-Pd-NCM-[Al]	0.02	1.40	20.0	1.5/91.6/6.9	93
C-Pd-NCM-[Al]	0.10	0.50	23.1	1.2/88.9/9.9	90
C-Pd-NCM-[Al]	0.02	0.50	40.0	1.0/92.0/7.0	93
C-Pt-NCM-[Al]	0.10	1.73	5.0	1.6/82.7/15.7	84
C-Pt-NCM-[Al]	0.02	1.73	11.3	1.4/83.8/14.8	85
A-Pd-NCM-[AlSi]	0.10	0.55	3.8	1.0/83.2/15.8	84
A-Pd-NCM-[AlSi]	0.02	0.55	5.6	1.5/84.7/13.8	86
C-Pt-NCM-[AlSi]	0.10	1.73	1.9	1.6/57.1/41.3	58
Pd/Al_2O_3[c]	0.10	0.50	15.6	1.3/93.8/4.9	95
Pd/Al_2O_3[c]	0.02	0.50	6.9	1.2/94.9/3.9	96

[a] Reaction conditions: 0.013 mol of DHL in 30 mL of 2-propanol at 70 °C and 960 shakes per minute (without diffusion limitations). [b] DiHL (dihydrolinalool) is the fully hydrogenated compound. [c] Pd/Al_2O_3 (0.5% Pd) obtained from Degussa AG.

Table 3. Catalytic Activity and Selectivity of Pd-NCM-Templated Mesoporous Alumina in Hydrogenation of DMEC to DMVC[a]

catalyst notation	catalyst amount, g	elemental analysis data on metal, %	specific rate, mol mg of Pd^{-1} min^{-1}	product ratio, wt. % DMEC/DMVC/MB[b]	selectivity, %
C-Pd-NCM-[Al]	0.1	0.50	31.3	1.3/88.8/9.9	90
C-Pd-NCM-[Al]	0.02	0.50	38.1	1.5/90.6/7.9	92
A-Pd-NCM-[Al]	0.10	1.40	13.1	1.2/85.0/13.8	86
A-Pd-NCM-[Al]	0.02	1.40	25.6	1.0/90.1/8.9	91
A-Pd-NCM-[AlSi]	0.10	0.55	16.9	1.6/83.6/14.8	85
Pd/Al_2O_3[c]	0.10	0.50	8.1	1.1/92.0/6.9	93

[a] Reaction conditions: 0.013 mol of acetylene alcohol in 30 mL of 2-propanol at 70 °C and 960 shakes per minute (without diffusion limitations). [b] MB (2-methylbutanol-2) is the fully hydrogenated compound. [c] Pd/Al_2O_3 (0.5% Pd) obtained from Degussa AG.

via oxygen).[36] The absence of silanol groups is supported by similarity of the ^1H NMR spectra of MNCM-templated alumina and aluminosilica (Figure 5d shows ^1H NMR of A-Pd-NCM-[AlSi]). They contain two main resonances at 0 and 2.5 ppm, which can be assigned to Al−O−H and Al−O−H···O, respectively, in $Al_3O(OH)_9^{2-}$ triclusters.[37]

As the fraction of tetrahedral aluminum species in MNCM-templated aluminosilica and especially alumina is low, one could expect low acidity of these materials. In fact, as these materials containing Pd and Pt nanoparticles are designed as catalysts for hydrogenation of acetylene alcohols, the lower the acidity (or the higher the basicity) of the support (here, alumina and aluminosilica), the more favorable the support for suppressing the side reactions.[38−40] To probe acidity and the nature of the acid sites of MNPM-templated aluminosilica and alumina, FT-IR has been used with pyridine as a probe molecule. When pyridine is protonated on a Brønsted acid site, the characteristic vibration at 1540 cm^{-1} appears in the IR spectrum.[41] When pyridine is coordinated to a Lewis acid site, it produces a band between 1447 and 1460 cm^{-1},[42] although other authors[43] report the appearance of several IR bands in the spectral region 1700−1400 cm^{-1} responsible for Lewis acid sites of different strengths. As the spectra of the MNCM-templated alumina and aluminosilica did not show any bands that might be assigned to pyridine adsorption, spectra are not shown. Since both MNCM-templated alumina and aluminosilica are characterized by negligible acidity, both should be equally effective as hydrogenation catalysts.

Catalytic Properties in Hydrogenation of Acetylene Alcohols. The catalytic properties of Pd- and Pt-NCM-templated aluminosilicas and aluminas were studied in partial hydrogenation of acetylene alcohols. Table 2 presents catalytic data for MNCM-templated nanoporous solids in hydrogenation of DHL (acetylene alcohol C_{10}). One can see that aluminosilica-based samples (containing both Pd and Pt nanoparticles) show low selectivity (hydrogenation of triple and double bonds occurs practically simultaneously) and very low catalytic activity (expressed as a specific rate). The latter is rather unusual for Pt catalysts, which normally display high activity and low selectivity in hydrogenation of a triple bond to a double bond.[44] In the case of Pd nanoparticles embedded in the aluminosilica samples, low activity along with *low selectivity* (Pd nanoparticles are normally quite selective in hydrogenation[44]) can be explained by restrictions for substrate transport inside the aluminosilica pores (the material has low mesoporosity and high microporosity). Probably, nanoparticles are barely accessible for DHL molecules, which destroys the activity. On the other hand, too slow desorption from the nanoparticles surface due to high diffusion limitations in the small pores suppresses the selectivity of the catalysts. When DHL is replaced with a smaller substrate, DMEC, catalyst activity increases, as diffusion limitations are less pronounced for shorter DMEC (Table 3). In the same vein, diffusion limitations of a longer substrate, DHIP, in the aluminosilica pores should be more prominent, which is reflected in lower activity.

(36) Debras, G.; Nagy, J. B.; Gabelica, Z.; Bodart, P.; Jacobs, P. A. *Chem. Lett.* **1983**, 199.
(37) Xue, X.; Kanzaki, M. *J. Phys. Chem. B* **2001**, *105*, 3422.
(38) Pellet, R. J. *J. Catal.* **1998**, *177*, 40.
(39) Grau, R. J.; Zgolicz, P. D.; Gutierrez, C.; Taher, H. A. *J. Mol. Catal. A* **1999**, *148*, 203.
(40) Scire, S.; Crisafulli, C.; Maggiore, R.; Minico, S.; Galvagno, S. *Appl. Surf. Sci.* **1998**, *136*, 311.
(41) Biz, S.; White, M. G. *J. Phys. Chem. B* **1999**, *103*, 8432.
(42) Hughes, T. R.; White, H. M. *J. Phys. Chem.* **1967**, *71*, 2192.
(43) Liu, X.; Truitt, R. E. *J. Am. Chem. Soc.* **1997**, *119*, 9856.
(44) Guo, X.-C.; Madix, R. J. *J. Catal.* **1995**, *155*, 336.

Table 4. Catalytic Activity and Selectivity of MNCM-Templated Nanoporous Alumina and Aluminosilica in Hydrogenation of DHIP to IP[a]

catalyst notation	catalyst amount, g	elemental analysis data on metal, %	specific rate, mol mg of Pd^{-1} min^{-1}	product ratio, wt. % DHIP/IP/DiHIP[b)]	selectivity, %
C-Pd-NCM-[Al]	0.10	0.50	21.9	1.5/96.5/2.0	98
C-Pd-NCM-[Al]	0.02	0.50	12.5	1.3/95.7/3.0	97
A-Pd-NCM-[Al]	0.10	1.40	16.3	1.0/89.1/9.9	90
A-Pd-NCM-[Al]	0.02	1.40	13.1	1.2/87.9/10.9	89
A-Pd-NCM-[AlSi]	0.10	0.55	2.5	1.1/85.1/13.8	86
Pd/Al_2O_3[c]	0.10	0.50	8.1	1.3/91.8/6.9	93

[a] See reaction conditions for Table 2. [b] DiHIP (dihydroisophitol) is the fully hydrogenated compound. [c] Pd/Al_2O_3 (0.5% Pd) obtained from Degussa AG.

For catalysts based on mesoporous alumina, the situation is quite different. Here, the fraction of mesopores is much higher, which allows DHL molecules to move along the pore channels. Increase of specific activity and selectivity when the catalyst amount decreases shows that excess of reaction sites allows both DHL and LN to coordinate with Pd which decreases both selectivity and activity as not all reaction sites are used by DHL molecules. As the structure of aluminum sites in both A-Pd-NCM-[Al] and C-Pd-NCM-[Al] catalysts is the same (according to ^{27}Al NMR data), the support influence should also be similar. The higher activity of C-Pd-[Al] can be explained by a lower fraction of the large particles and lower Pd content compared to A-Pd-NCM-[Al]. The latter factor allows one to avoid shielding of the particle surface due to other particles located in its vicinity. When a shorter substrate is used (C_5), the same trend is observed (Table 3): higher activity with C-Pd-NCM-[Al] catalyst than with A-Pd-NCM-[Al].

At the same time, for C_{20} alcohol hydrogenation, the difference in activity between the above catalysts is rather negligible, but in selectivity is pronounced (Table 4). The higher selectivity of C-Pd-NCM-[Al] can be explained by the much higher pore size, which prevents diffusion limitations for C_{20} acetylene alcohol molecules and facilitates desorption and removal of isophytol (hydrogenation product) from the Pd particle surface. This prevents further hydrogenation of isophytol, resulting in the decreased selectivity. Here, a decrease of the catalyst amount leads to a decrease of activity (contrary to the shorter substrates, DHL and DMEC). This fact can be explained by taking into account the relative sizes of the substrates and the active sites.[45] For steric reasons, only a portion of the Pd atoms can be catalytically active at one time, that is, several atoms form an active site where substrate adsorption and catalytic reaction takes place. Consistent with this, each substrate, when adsorbed on the active site, occupies a certain area on the catalyst surface. In accordance with ref 46, comparing the Pd atom diameter and the spatial demand of reactive molecules, DHL (or substrate of a similar size) should occupy an active site consisting of at least 7 atoms (1 central atom with 6 atoms surrounding the central one). For DHIP, which contains 20 carbon atoms, the active site may contain more Pd atoms (supposedly 19, if two layers of Pd atoms are located around the central atom). As a result, to obtain the same amount of active centers and to achieve the highest activity, more Pd atoms (higher catalyst amount) should be provided.

Thus, the C-Pd-NCM-[Al] catalyst allows reaching the high selectivity for DHIP hydrogenation at a reasonable catalyst activity. These values are especially striking in comparison with a commercial Pd/A_2O_3 catalyst (Table 4). When this catalyst was modified with Pb acetate, pyridine, and alkali, selectivity increased to 97−98%, but a specific rate (measure of activity used in this paper) was only 3.1 mol mg of Pd^{-1} min^{-1}.[47] DHIP hydrogenation with Lindlar catalyst ($Pd/CaCO_3$ modified with quinoline or Cu^{2+}, Cd^{2+}, Mn^{2+}, Fe^{3+}, and Co^{2+} ions) also results in a selectivity increase to 97.2−98.0%, but activity is nearly halved[48] compared to that with the nonmodified Pd/Al_2O_3 catalyst (see Table 4). Thus, the advantages of the C-Pd-NCM-[Al] catalyst in DHIP hydrogenation are high selectivity, much higher activity than for the above catalysts without using the additional modifiers which might pollute the final product and be hazardous for the environment.

Conclusion

Pd and Pt nanoparticles formed in cationic and anionic microgels derived from sulfonated polystyrene and poly(ethylmethacryltetramethylammonium chloride) can be embedded in nanoporous aluminosilica and alumina if the corresponding microgels are used as templates along with amphiphilic block copolymer. Metal particles stay intact after the calcination procedure. If the overall structure of Pd- and Pt-containing aluminosilica resembles the metal-containing silica cast over the microgel templates, the mesoporous alumina containing PdO and Pt nanoparticles is different and consists of an interpenetrating pore system and alumina nanowires (2−3 nm in diameter and about 40 nm in length). Both components are intimately mixed. According to the ^{27}Al MAS NMR spectra, alumina samples, independent of microgel and metal particle types, contain mainly six-coordinated Al species which are normally responsible for low acidity of mesoporous solid. The latter factor is favorable for hydrogenation reaction.

Catalytic properties of Pd- and Pt-containing aluminosilicas and aluminas were studied in selective hydrogenation of long-chain acetylene alcohols (C_5, C_{10}, C_{20}). Aluminosilica samples exhibited high activity and selectivity for neither substrate, which is probably caused by high diffusion limitations within pores. As might be

(45) Besson, M.; Blanc, B.; Champelet, M.; Gallezot, P.; Nasar, K.; Pinel, C. *J. Catal.* **1997**, *170*, 254.
(46) Niessen, H. G.; Eichhorn, A.; Woelk, K.; Bargon, J. *J. Mol. Catal. A: Chem* **2002**, *182*−*183*, 463.
(47) Sulman, E. M. *Russ. Chem. Rev.* **1994**, *63*, 923.
(48) Rajaram, J.; Narula, A. P. S.; Chawla, H. P. S.; Dev, S. *Tetrahedron* **1983**, *39*, 2315.

expected, the shorter the substrate, the higher the activity, so the highest activity was achieved for DMEC (C_5). Mesoporous alumina cast over cationic microgels with Pd nanoparticles displayed a high selectivity toward the longest acetylene alcohol, DHIP, along with satisfactory activity. Presumably, for DHIP, a perfect correlation between pore, nanoparticle, and substrate sizes is achieved. We believe that C-Pd-NCM-[Al] can be an excellent catalyst for other reactions as well, involving substrates of a similar size or structure.

Acknowledgment. The present work was supported by the NATO Science for Peace Programme (Grant SfP-974173) and Russian Foundation for Basic Research (Grant RFBR-01-03-32937). We sincerely thank Jan H. Schattka for help with BET measurements.

CM021776X